

Copy No. 148

RM No. L8H25

**RESTRICTED**

NACA RM No. L8H25



# **RESEARCH MEMORANDUM**

CLASSIFICATION CHANGED TO

UNCLASSIFIED

AUTHORITY CROWLEY CHANGE #2003

DATE 12-14-53 T.C.F.

STATIC LONGITUDINAL AERODYNAMIC CHARACTERISTICS  
OF A 52° SWEPTBACK WING OF ASPECT RATIO 2.88 AT REYNOLDS  
NUMBERS FROM 2,000,000 TO 11,000,000

By

James E. Fitzpatrick and Gerald V. Foster

Langley Aeronautical Laboratory  
Langley Field, Va.

CLASSIFIED DOCUMENT

This document contains classified information affecting the National Defense of the United States within the meaning of the Espionage Act, USC 7931 and 32. Its transmission or the revelation of its contents in any manner to unauthorized person is prohibited by law. Information so classified may be imparted only to members of the military and naval services of the United States, appropriate civilian officers and employees of the Federal Government who have a legitimate interest therein, and to United States citizens of known loyalty and discretion who of necessity must be informed thereof.

**NATIONAL ADVISORY COMMITTEE  
FOR AERONAUTICS**

WASHINGTON

November 16, 1948

**RESTRICTED**



## NATIONAL ADVISORY COMMITTEE FOR AERONAUTICS

## RESEARCH MEMORANDUM

## STATIC LONGITUDINAL AERODYNAMIC CHARACTERISTICS

OF A  $52^{\circ}$  SWEPTBACK WING OF ASPECT RATIO 2.88 AT REYNOLDS

NUMBERS FROM 2,000,000 TO 11,000,000

By James E. Fitzpatrick and Gerald V. Foster

## SUMMARY

The effects of changes in Reynolds number on the longitudinal aerodynamic characteristics of a  $52^{\circ}$  sweptback wing with an aspect ratio of 2.88 and NACA 64<sub>1</sub>-112 airfoil sections were investigated. The range of Reynolds numbers was from 2,000,000 to 11,000,000. The model was tested with the leading edge both smooth and rough. The tests also included a study of the flow changes at moderate to high lift coefficients.

Abrupt changes in the variations of the forces and moments were observed at moderate lift coefficients; that is, the lift-curve slope became higher, the pitching-moment curve became more stabilizing and the drag suddenly increased. These changes were coincident with separation around the tip leading edge. As the angle of attack was further increased, the pitching-moment curve broke in a destabilizing direction at the point of initial lift-curve-slope reduction.

The lift coefficient at which the initial changes in the force and moment variations occurred for the smooth wing increased markedly with Reynolds number. Roughness reduced the influence of Reynolds number on this lift coefficient for Reynolds numbers beyond 3,600,000.

A maximum lift coefficient of 1.12 was attained on the plain wing at the highest Reynolds number of the test, an increase of only 0.03 over that obtained at the lowest Reynolds number. The addition of split flaps did not appreciably increase the maximum lift coefficient.

Roughness on the leading edge reduced the lift coefficient at which the force and moment variations suddenly changed but had little influence on the maximum lift coefficient.

The lift-curve slope through zero lift was slightly higher than would be indicated by the swept-lifting-line theory of Weissinger. Good agreement was also obtained between the calculated and experimentally determined values of aerodynamic-center location.

## INTRODUCTION

As demonstrated in reference 1, a sweptback wing is characterized by a stalling pattern in which boundary-layer separation starts near the tip and causes longitudinal instability for certain aspect ratios near maximum lift. Because the constitution of the boundary layer depends upon the Reynolds number, a general inquiry into the aerodynamic properties of swept wings is at present being conducted in the Langley 19-foot pressure tunnel through a relatively large range of Reynolds numbers. As a part of this study, an investigation was made of the longitudinal aerodynamic characteristics of a 52° sweptback wing of aspect ratio 2.88.

The tunnel dynamic pressure was varied to maintain several values of Reynolds number from 2,000,000 to 11,000,000, both with and without 50-percent-span split flaps and with the model leading edge both smooth and rough.

## COEFFICIENTS AND SYMBOLS

$C_L$  lift coefficient ( $L/qS$ )

$C_D$  drag coefficient ( $D/qS$ )

$C_m$  pitching-moment coefficient ( $M/q\bar{c}S$ )

$R$  Reynolds number ( $\rho V \bar{c} / \mu$ )

$L$  lift, pounds

$D$  drag, pounds

$M$  pitching moment about the quarter-chord point of the mean aerodynamic chord, pound-feet

$q$  free-stream dynamic pressure  $\left( \frac{1}{2} \rho V^2 \right)$ , pounds per square foot

$S$  wing area, square feet

$\bar{c}$  wing mean aerodynamic chord  $\left( \frac{2}{S} \int_0^{b/2} c^2 dy \right)$ , feet

$c$  local chord parallel to plane of symmetry, feet

$y$  spanwise coordinate, feet

V	free-stream velocity, feet per second
$\rho$	mass density of air, slugs per cubic foot
$\mu$	coefficient of viscosity of air, slugs per foot-second
$\alpha$	angle of attack, degrees
$\Lambda$	angle of sweepback, degrees

### MODEL

The plan form of the wing and principal dimensions are shown in figure 1. The wing had an angle of sweepback of  $52^\circ$  at the leading edge, an aspect ratio of 2.88, a taper ratio of 0.625, and NACA 64-112 airfoil sections perpendicular to the 0.282-chord line. It was constructed of laminated mahogany and is believed to have remained rigid enough to eliminate the effects of aeroelastic distortion. The 0.282-chord line corresponded to the quarter-chord line of the wing panels before they were swept back. The tips were rounded off in both plan form and elevation beginning at  $0.975\frac{b}{2}$ . The wing had no geometric dihedral or twist.

The installation and geometry of the 50-percent-span, 20-percent-chord split flaps are shown in figure 1.

A leading-edge roughness was obtained by applying No. 60 (0.011-inch mesh) carborundum grains to a thin layer of shellac over a surface length of 8 percent chord measured from the leading edge normal to the 0.282-chord line on both upper and lower surfaces. The grains covered 5 to 10 percent of the affected area.

### TESTS

The tests were conducted in the Langley 19-foot pressure tunnel. Figure 2 depicts the model installed in the tunnel test section on the normal support system. Measurements of lift, drag, and pitching moment were made through a range of angle of attack from  $-4^\circ$  to  $28^\circ$ . The model was tested both with and without half-span split flaps and leading-edge roughness through a range of Reynolds numbers from 2,000,000 to 9,700,000. An additional test was made at a Reynolds number of 11,000,000 for the plain wing. The total range of Mach number was from 0.08 to 0.21.

Studies of the stall progression were made at a Reynolds number of 3,600,000 and 6,800,000 by observations of wool tufts attached to the upper surface of the wing. An attempt was made to study further the flow

changes evident at moderate to high lift coefficients. Accordingly, tufted masts 8 inches high were placed on the upper surface 85 percent of the semispan from the plane of symmetry at the 10-, 30-, 50-, and 70-percent-chord stations. Threads were also attached to the wing leading edge at ten spanwise stations and their motions observed. In addition, the core of the edge trailing vortex was found by means of a three-tuft probe at several longitudinal stations. For each point the probe was lowered until the center tuft was in the center of the vortex, the bottom tuft assumed one direction, and the third tuft was blown in the opposite direction. The probe was then raised until the center tuft also assumed a definite direction. The probe was then lowered until the center tuft assumed the opposite direction. This procedure was followed as the probe was returned to the center and then displaced right and left. The center of these four positions defined the vortex core with satisfactory accuracy.

## RESULTS AND DISCUSSION

The data presented herein have been corrected for the effects of model-support tare and interference and for air-stream misalignment. Jet-boundary corrections were determined according to the method of reference 2 for the angle of attack and drag coefficient. The pitching-moment coefficient has been corrected for wing-loading distortion resulting from tunnel restriction.

### Force and Pitching-Moment Results

The wing characteristics of lift, drag, and pitching moment are presented in figures 3 to 5 for both the smooth and rough conditions. A significant peculiarity of these data is the inflections in the lift, drag, and especially in the pitching-moment curves at moderate lift coefficients (figs. 3 to 5).

The lift curves have a linear slope of 0.047 from low to moderate lift coefficients, followed by an increase in slope and then a reduction as the angles of attack become larger. At lift coefficients beyond the inflection, a rapid increase in drag is noted (fig. 5) and the stabilizing slopes of the pitching-moment curves increase (figs. 3 and 4). At slightly higher lift coefficients, an unstable break occurs in the pitching-moment curves and the lift-curve slope is reduced due to tip stalling. This type of lift, drag, and pitching-moment curve has been observed for other low-aspect-ratio, highly swept wings (references 1 and 3). The force and moment breaks of figures 3 to 5, however, display a pronounced variation with Reynolds number. As pointed out in reference 4, sudden changes in the variations of effective dihedral and directional stability also begin at the lift coefficient at which the inflections occur in the data of figures 3 and 4. The lift coefficient

at which initial separation occurs has been observed to be almost identical with the inflection point. The variation of this inflection lift coefficient with Reynolds number (fig. 6(a)) might thus be considered a primary scale effect.

The maximum lift coefficient of the wing was 1.09 at a Reynolds number of 2,000,000 (fig. 6(b)). A negligible increase in maximum lift coefficient was realized with an increase in Reynolds number to 11,000,000. With the rough leading edge, both the increase in slope of the lift curve and the reduction that followed occurred at a lower lift coefficient than that of the smooth wing and there was little scale effect except at Reynolds numbers below 3,600,000 (fig. 6(a)). A similar variation was noted at the lift coefficient at which the pitching moment became destabilizing. The reduction in  $C_{L_{max}}$  due to roughness was small. The addition of semispan split flaps did not appreciably increase the maximum lift coefficient at any of the Reynolds numbers (fig. 6(b)). The split flaps, however, did delay the onset of the inflection by  $\Delta C_L$  of about 0.17 (fig. 6(a)). Roughness tended to minimize the severity of the inflection when the flaps were deflected even more than when the flaps were neutral.

#### Flow Observations

Tuft indication.— As shown in figure 7, at a Reynolds number of 3,600,000, there was no appreciable change in the flow over the wing until an angle of attack of  $12.7^\circ$  was reached. At  $14.8^\circ$ , separation was indicated at the leading edge near the tip. Between angles of attack of  $14.8^\circ$  and  $15.9^\circ$  there was a large change in the flow over the outboard portion of the wing. At  $15.9^\circ$ , separation around the leading edge was indicated by the four outboard leading-edge threads which were raised from the surface and described a circular motion (fig. 7). The remainder of the surface tufts on the outer third of the wing were disturbed and indicated a spanwise flow. The bottom tuft on the front mast and the lower two tufts on the second mast were twisted around their respective masts also indicating a radical flow change. The flow changes just described occurred approximately  $1^\circ$  earlier on the left wing panel than on the right. Referring to the force data, it is seen that the initial force and moment changes occur concurrently with the separation around the leading edge at this Reynolds number. Increasing the Reynolds number delayed the initial separation, as shown by comparing figures 7 and 8. As the angle of attack is increased the leading-edge separation spreads inboard, and separated flow appears behind the leading edge, gradually progressing inboard and chordwise.

Trailing-vortex-core locations.— At a Reynolds number of 3,600,000, the trailing-vortex core was located at several longitudinal stations. Surveys made at lift coefficients well below the inflection indicate the trailing vortex to be formed in the normal manner. It is shown in figure 9, however, to be above the wing-tip region at a lift coefficient

just after the inflection point. The appearance of the trailing vortex over the wing concurrently with the inflection lift coefficient might lead to the supposition that, although the trailing vortex is formed in the normal manner at low lift coefficients, at the inflection lift coefficient the trailing vortex is formed by a gradual coalescence of the vortices indicated by the leading-edge separation shown in figure 7. A similar unusual trailing-vortex formation was described in references 5 and 6.

#### Discussion of Force and Moment Characteristics

As has been shown in reference 7, the lift coefficient at which incipient separation occurs on a yawed infinite wing is lower by the factor  $\cos^2\Lambda$  than the corresponding lift coefficient for an unyawed wing, if the Reynolds number and airfoil are the same normal to the leading edge. The inflection lift coefficient (0.8) of the present wing at a Reynolds number of 11,000,000 is considerably greater than the point of initial separation estimated for a yawed infinite wing (0.6). Tests reported in reference 8 also show that decreasing the aspect ratio increases the lift coefficient at which the inflections in the force and moment curves first appear. These results indicate that finite span effects are considerable in modifying the airfoil section characteristics. The free vortex observed above the tip of the present wing may be a contributing factor to the occurrence of the inflection in the force and moment curves, inasmuch as this type of vortex has been known to cause large changes in the airfoil pressure distribution (reference 5).

The pitching-moment curves of figures 3 and 4 show a rearward movement of the aerodynamic center at the inflection lift coefficient. The motion of the outboard leading-edge threads when the inflection occurs, moreover, indicates separation and possibly the formation of trailing vortices similar to those reported on triangular plates in reference 5. The action of the vortex flow over the outer part of the wing could be a factor in changing the lift- and moment-curve slopes. The large increase in drag that occurs at the inflection lift coefficient is attributed in part to the reduction of the suction pressures at the leading edge near the tip. The wing had a high enough sweep so that a small increase in lift and drag near the tip would have a substantial effect on the pitching moment.

The longitudinal instability at higher angles of attack is attributed to the expanding regions of completely separated flow near the tip, which decrease the relative lift load carried outboard. Further studies, particularly detailed pressure measurements, are needed to describe adequately the flow over the wing in the nonlinear range.

Comparison with the 42° sweptback wing.—The results of scale-effect tests of a 42° sweptback wing of aspect ratio 4 are presented in reference 9. At the higher Reynolds numbers these results are considerably different from those presented herein. When separation was first apparent near the tip of the 42° sweptback wing, a reduction in lift resulted and the pitching-moment curve broke in an unstable direction, whereas an increase in lift and drag and a stabilizing break occurred on the 52° sweptback wing. Separation on the 42° sweptback wing was manifested by a complete reversal of flow direction at the front surface over the entire outer panel, while on the 52° sweptback wing it was shown by a circular motion of leading-edge tufts indicating separation around the leading edge and subsequent reattachment further aft. At the minimum Reynolds number, however, the characteristics of the 42° sweptback wing are similar to those of the 52° sweptback wing herein presented.

The maximum lift coefficients of the two wings were approximately the same; however, a lower inflection lift coefficient was obtained on the 52° sweptback wing. The increment in  $C_{L_{max}}$  due to flaps was about 0.2 for the 42° sweptback wing, as compared with 0.025 for the present wing. The increment in force inflection  $C_L$  due to flaps, however, compares favorably with that of the 42° sweptback wing considering the greater sweep and lower aspect ratio.

Comparison with theory.—Below the inflection lift coefficient, the lift-curve slope can be fairly well predicted by the method of Weissinger (reference 10). The predicted lift-curve slope is 0.044, while the measured lift-curve slope is 0.047. This is an underestimation of about 6.4 percent which is good considering the simplifying assumptions of the theory.

The position of the aerodynamic center is, on the average, 0.25 mean aerodynamic chord. The theory predicts a position of 0.257 mean aerodynamic chord, including a correction for the effect of thickness, a discrepancy of only 0.7 percent mean aerodynamic chord.

The increment in lift due to split flaps was calculated by an adaptation of the method of reference 11 given in reference 12 as follows:

$$\Delta C_{L_{\alpha=0}} = J(\Delta C_L) (\cos \Lambda) C_{L_{\alpha \Lambda}}$$

where  $J$  is the factor depending on aspect ratio, taper ratio, and flap span given in reference 11;  $\Delta C_L$  is the increment in flap lift coefficient of the airfoil section; and  $C_{L_{\alpha \Lambda}}$  is the calculated lift-curve slope of the swept wing.

The preceding equation was an adaptation of a straight lifting-line theory to a wing of moderate sweep ( $35^\circ$ ) and normal aspect ratio (6). Its application to a wing of higher sweep ( $52^\circ$ ) and lower aspect ratio (2.88) might be somewhat presumptuous. Nevertheless, the calculated value was 0.24, the measured value 0.28, an underestimation of 14 percent.

#### SUMMARY OF RESULTS

The tests of a  $52^\circ$  sweptback wing of aspect ratio 2.88 lead to the following results:

1. Abrupt changes in the variations of the forces and moments were observed at moderate lift coefficients; that is, the lift-curve slope became greater, the pitching-moment curve became more stabilizing, and the drag suddenly increased. These changes were coincident with separation around the tip leading edge. As the angle of attack was further increased, the pitching-moment curve broke in a destabilizing direction at the point of initial lift-curve-slope reduction.
2. The lift coefficient at which these initial changes in the force and moment variations occurred (inflection lift coefficient) for the smooth wing increased markedly with Reynolds number. Roughness reduced the influence of Reynolds number on the inflection lift coefficient beyond a Reynolds number of 3,600,000.
3. A maximum lift coefficient of 1.12 was attained on the plain wing at the highest Reynolds number of the test, an increase of only 0.03 over that obtained at the lowest Reynolds number. The addition of split flaps did not appreciably increase the maximum lift coefficient.
4. Roughness caused a reduction in the value of the "inflection" lift coefficient but had no appreciable effect on the maximum lift coefficient. The lift coefficient at which the pitching-moment curve broke in the destabilizing direction was also reduced with roughness.
5. The lift-curve slope through zero lift is slightly higher than would be indicated by the swept lifting-line theory of Weissinger. Good agreement was also obtained between the calculated and experimental values of the aerodynamic-center location.

Langley Aeronautical Laboratory  
National Advisory Committee for Aeronautics  
Langley Field, Va.

## REFERENCES

1. Lowry, John G., and Schneiter, Leslie E.: Investigation at Low Speed of the Longitudinal Stability Characteristics of a  $60^{\circ}$  Swept-Back Tapered Low-Drag Wing. NACA TN No. 1284, 1947.
2. Eisenstadt, Bertram J.: Boundary-Induced Upwash for Yawed and Swept-Back Wings in Closed Circular Wind Tunnels. NACA TN No. 1265, 1947.
3. Lange and Wacke: Prüfbericht über 3- und 6-Komponentenmessungen an der Zuspitzungsreihe von Flügeln kleiner Streckung. Deutsche Luftfahrtforschung (Berlin-Adlershof), 1943.  
Teilbericht: Trapezflügel. UM Nr. 1023/1.  
Teilbericht: Ellipsenflügel. UM Nr. 1023/3. (Available as NACA TM No. 1146, 1947)  
Teilbericht: Dreieckflügel. UM Nr. 1023/5. (Available as NACA TM No. 1176, 1948.)
4. Salmi, Reino J.: Yaw Characteristics of a  $52^{\circ}$  Sweptback Wing of NACA 64<sub>1</sub>-112 Section with a Fuselage and with Leading-Edge and Split Flaps at Reynolds Numbers from  $1.93 \times 10^6$  to  $6.00 \times 10^6$ . NACA RM No. L8H12, 1948.
5. Winter, H.: Flow Phenomena on Plates and Airfoils of Short Span. NACA TM No. 798, 1936.
6. Wilson, Herbert A., Jr., and Lovell, J. Calvin: Full-Scale Investigation of the Maximum Lift and Flow Characteristics of an Airplane Having Approximately Triangular Plan Form. NACA RM No. L6K20, 1946.
7. Jones, Robert T.: Effects of Sweepback on Boundary Layer and Separation. NACA TN No. 1402, 1947.
8. Goodman, Alex, and Brewer, Jack D.: Investigation at Low Speeds of the Effect of Aspect Ratio and Sweep on Static and Yawing Stability Derivatives of Untapered Swept Wings. NACA TN No. 1669, 1948.
9. Neely, Robert H., and Conner, D. William: Aerodynamic Characteristics of a  $42^{\circ}$  Swept-Back Wing with Aspect Ratio 4 and NACA 64<sub>1</sub>-112 Airfoil Sections at Reynolds Numbers from 1,700,000 to 9,500,000. NACA RM No. L7D14, 1947.
10. DeYoung, John: Theoretical Additional Span Loading Characteristics of Wings with Arbitrary Sweep, Aspect Ratio, and Taper Ratio. NACA TN No. 1491, 1947.

11. Pearson, Henry A., and Anderson, Raymond F.: Calculation of the Aerodynamic Characteristics of Tapered Wings with Partial-Span Flaps. NACA Rep. No. 665, 1939.
12. Koven, William, and Graham, Robert R.: Wind-Tunnel Investigation of High-Lift and Stall-Control Devices on a  $37^{\circ}$  Sweptback Wing of Aspect Ratio 6 at High Reynolds Numbers. NACA RM No. L8D29, 1948.

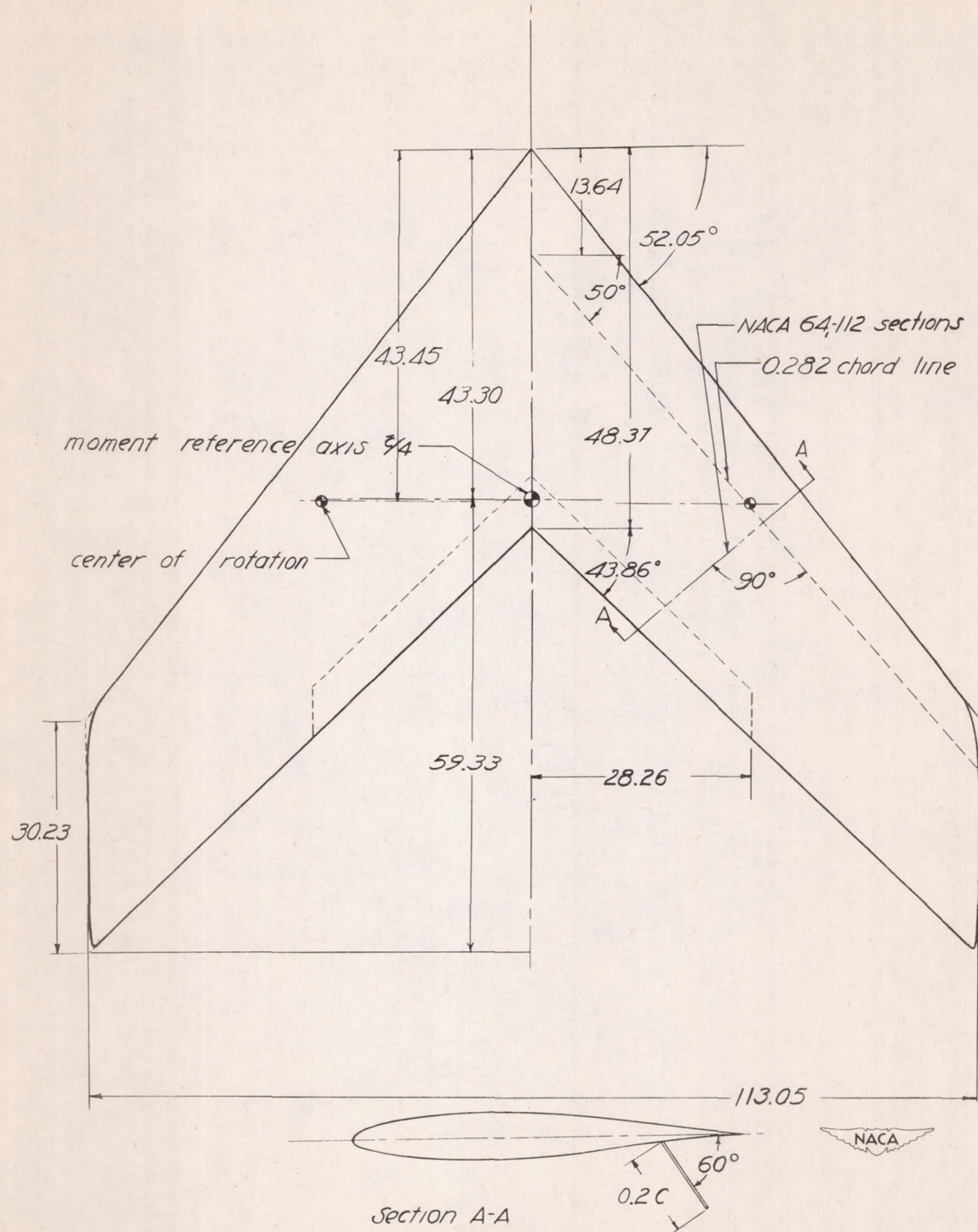


Figure 1.- Plan and section of  $52^{\circ}$  sweptback wing. Wing area = 4429 sq in.;  $\bar{c}$  = 39.97 in.; aspect ratio = 2.88. No twist. All dimensions in inches.



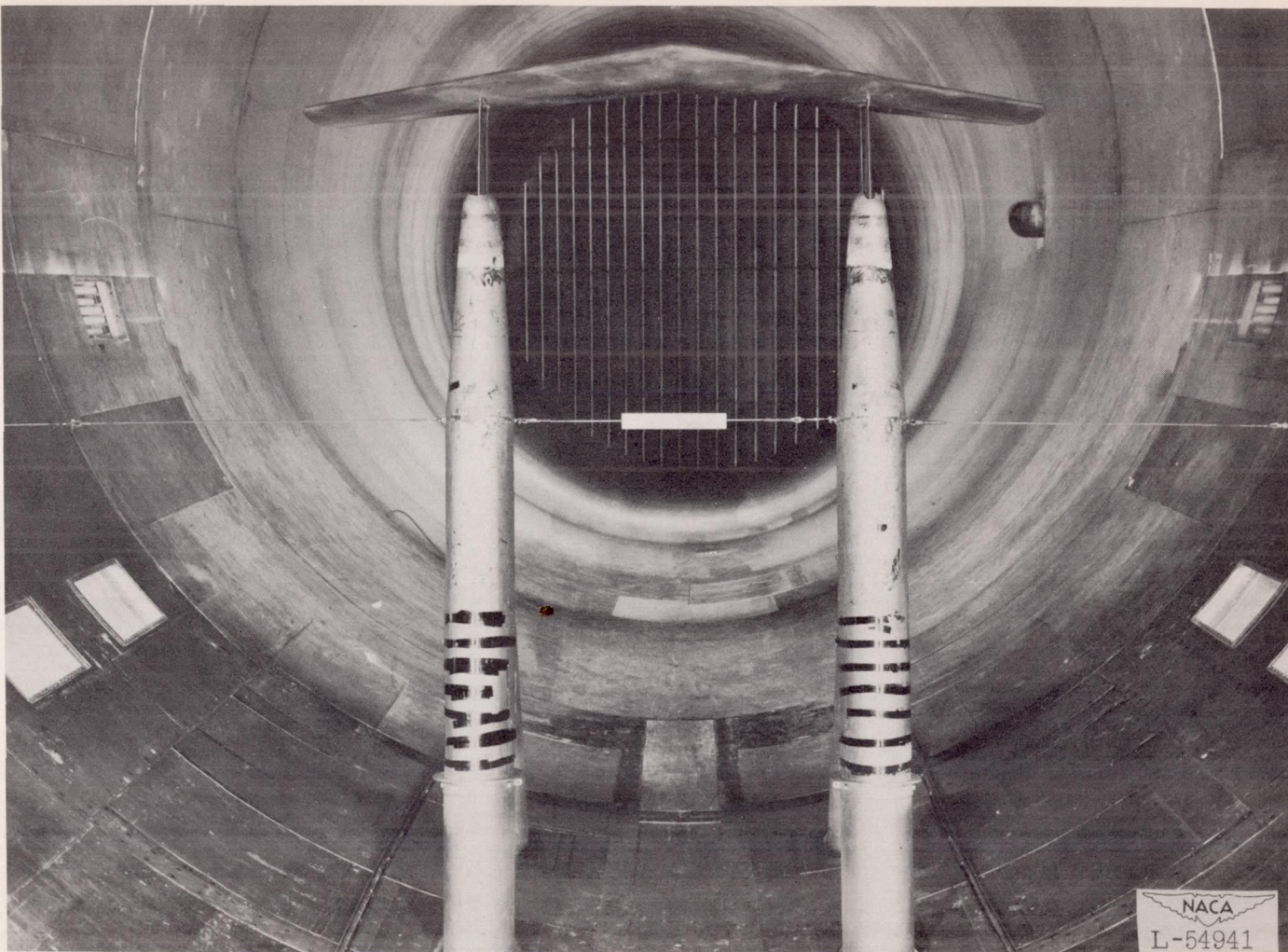
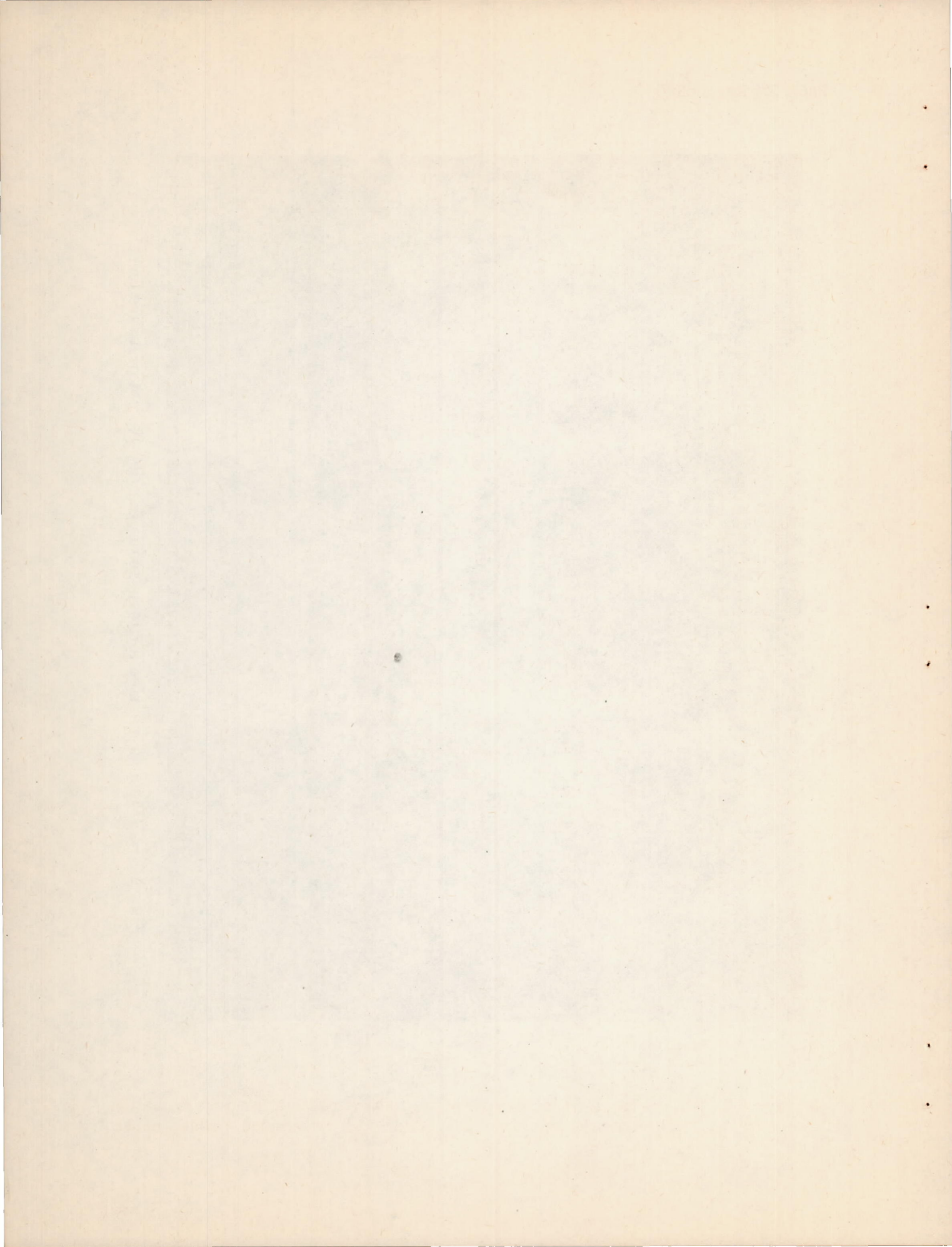


Figure 2.- Model as mounted for tests in the Langley 19-foot pressure tunnel.



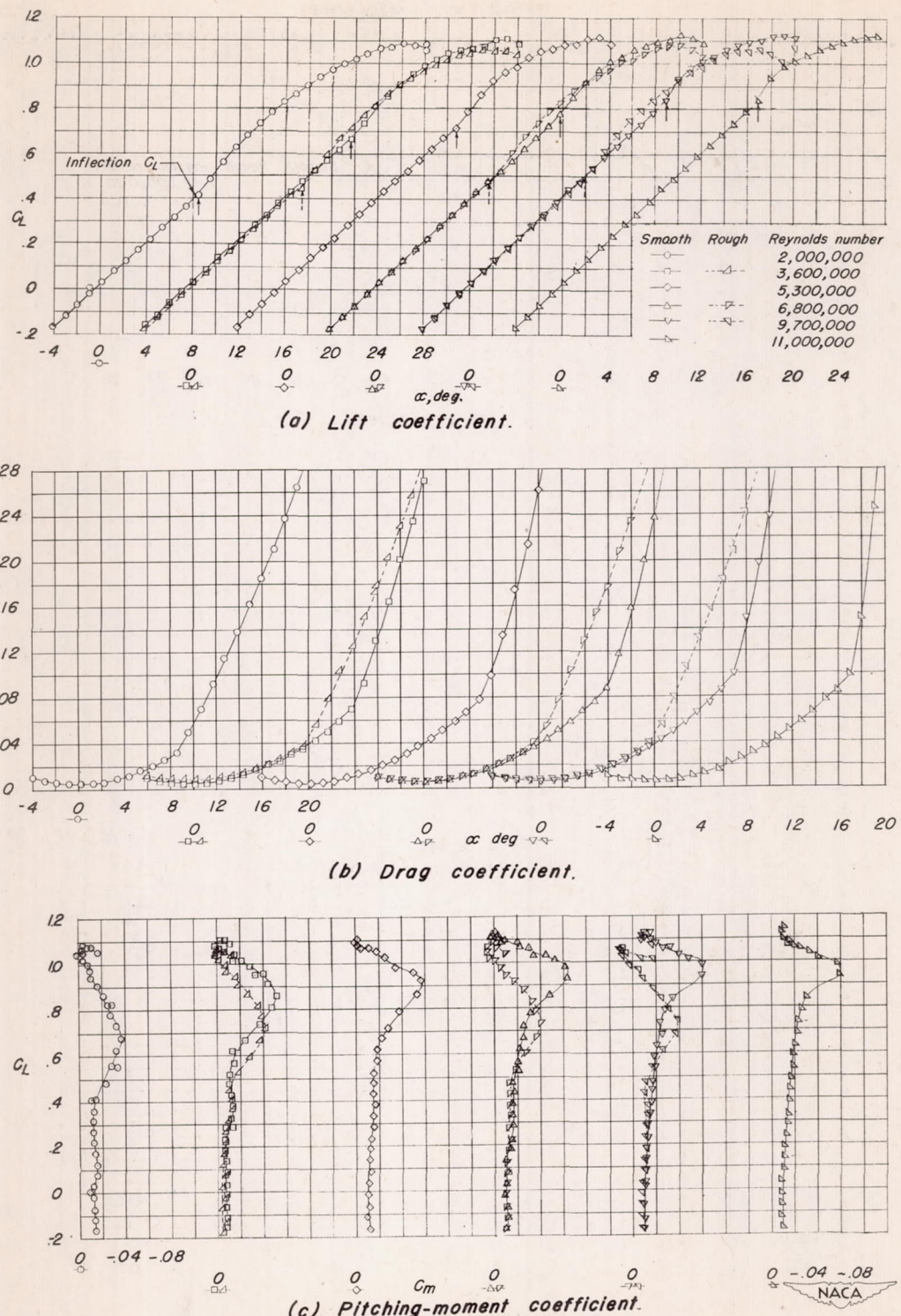
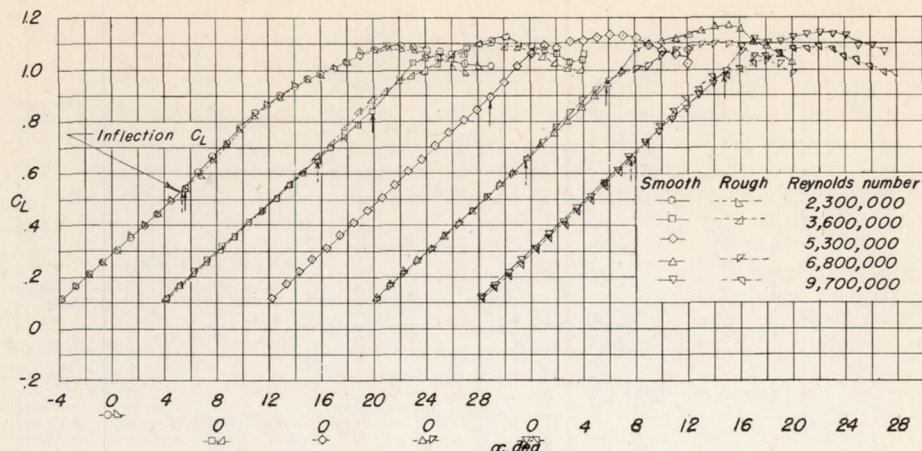
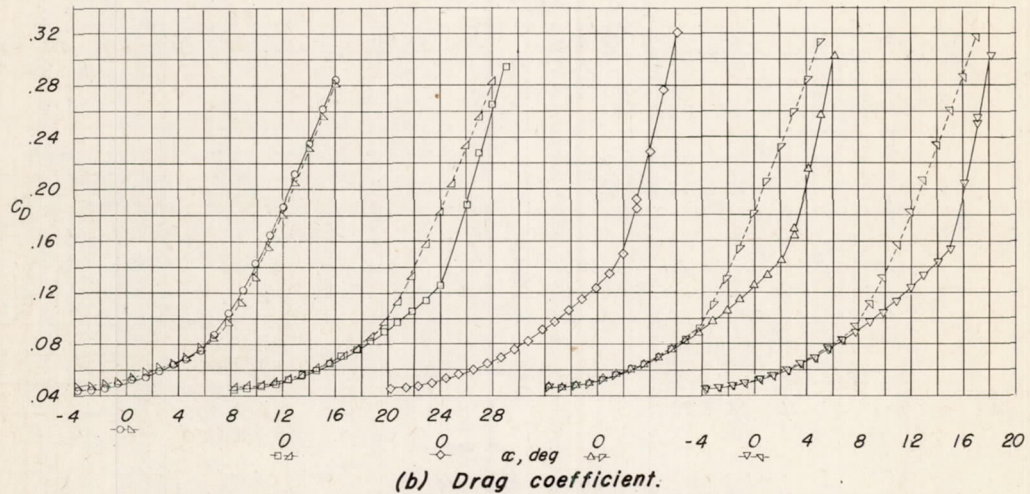


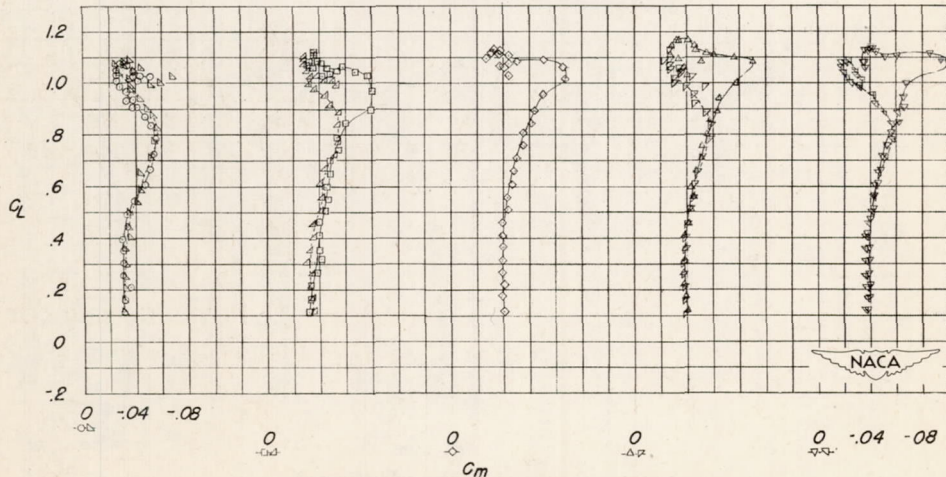
Figure 3.- Lift, drag, and pitching-moment characteristics for several values of Reynolds number with and without leading-edge roughness. Flaps neutral.



(a) Lift coefficient.

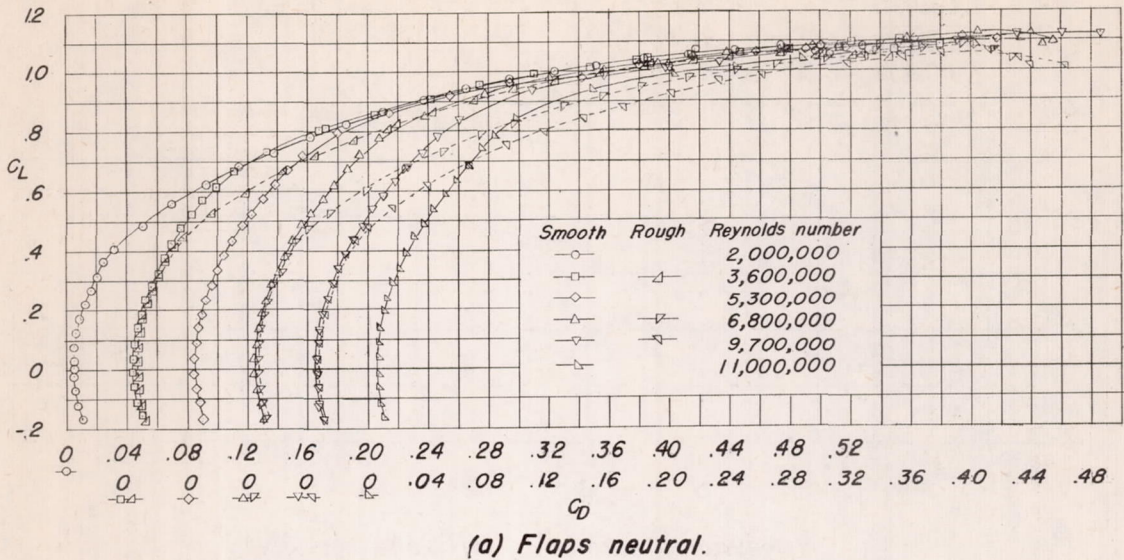


(b) Drag coefficient.

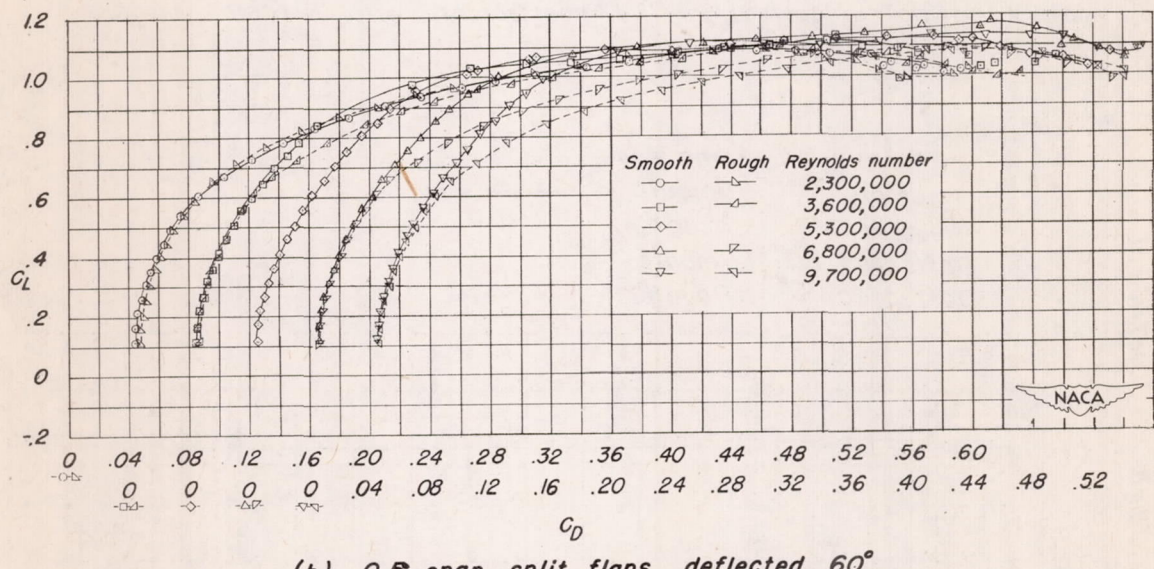


(c) Pitching-moment coefficient.

Figure 4.- Lift, drag, and pitching-moment characteristics for several values of Reynolds number with and without leading-edge roughness. 0.5-span split flaps deflected 60°.

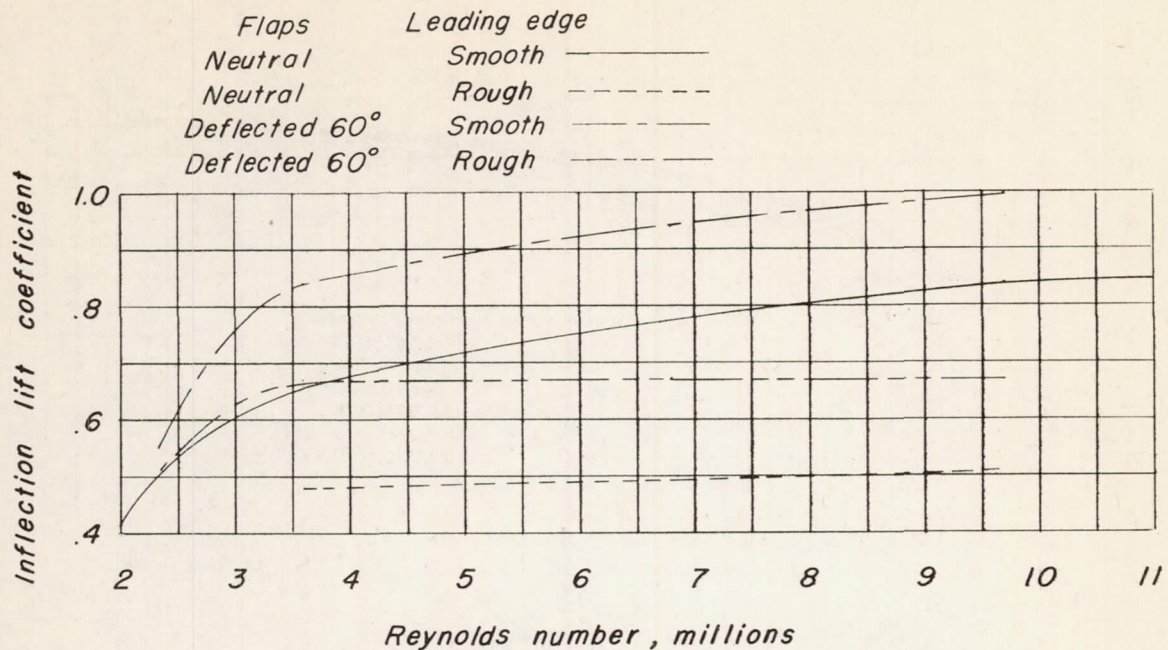


(a) Flaps neutral.

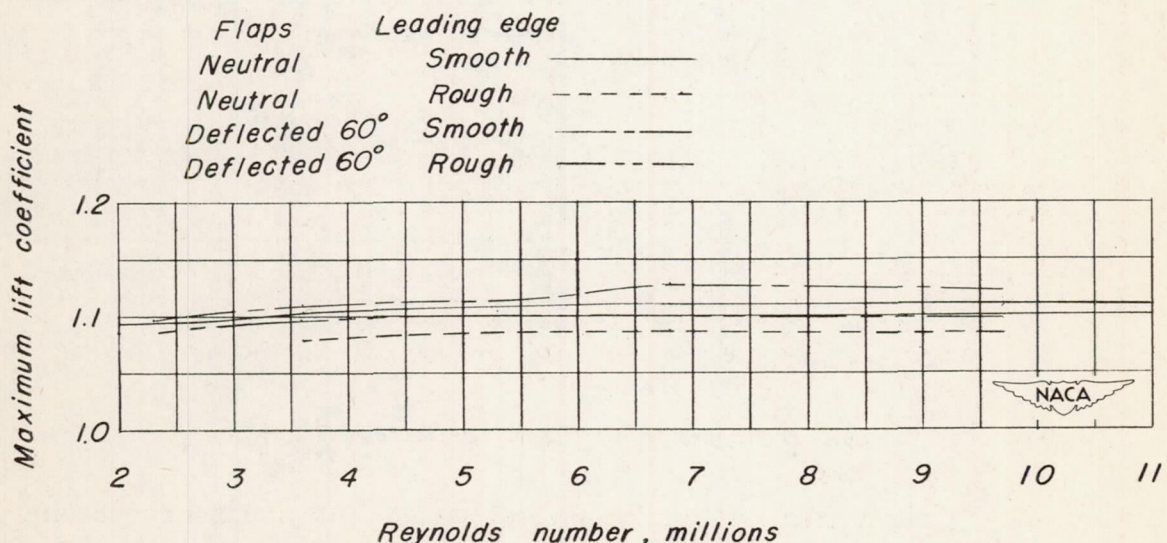


(b) 0.5-span split flaps deflected 60°.

Figure 5.- Drag characteristics for several values of Reynolds number with and without leading-edge roughness.



(a) Variation of inflection lift coefficient with Reynolds number.



(b) Variation of maximum lift coefficient with Reynolds number.

Figure 6.- Variations of maximum and inflection lift coefficient with Reynolds number. Flaps deflected or neutral, leading edge smooth or rough.

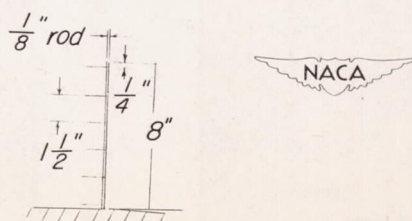
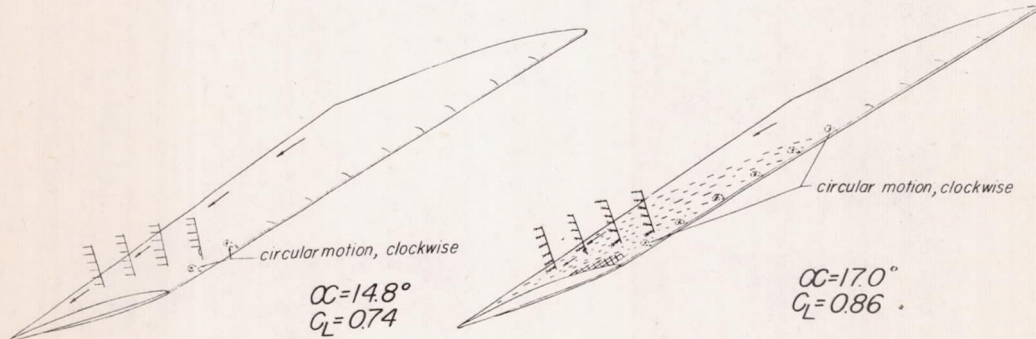
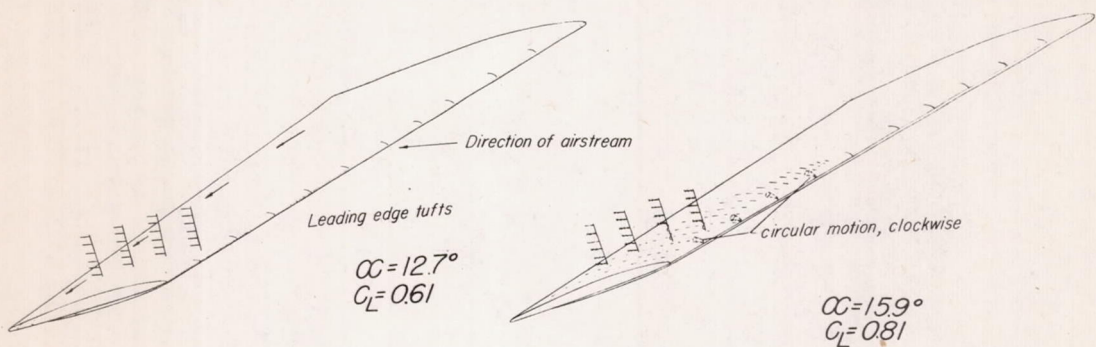
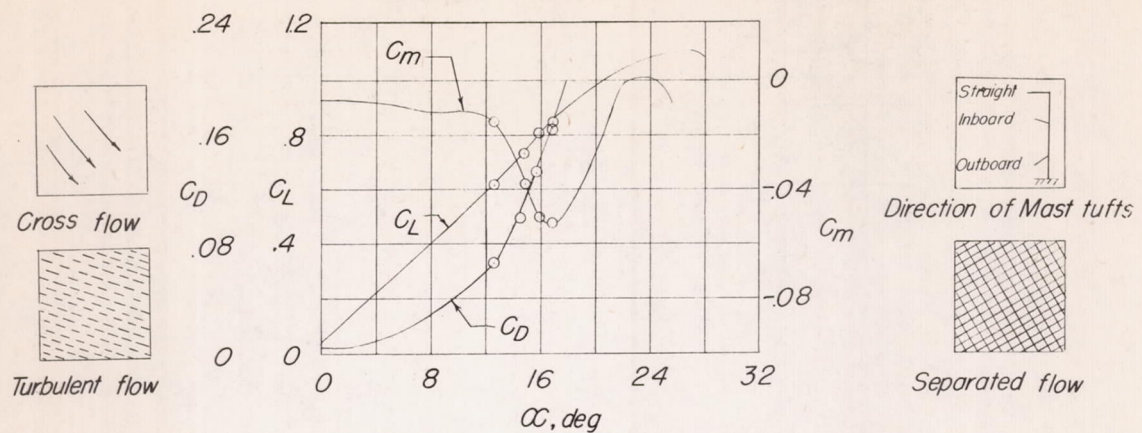


Figure 7.- Flow over the  $52^\circ$  sweptback wing;  $R = 3,600,000$ ; flaps neutral.

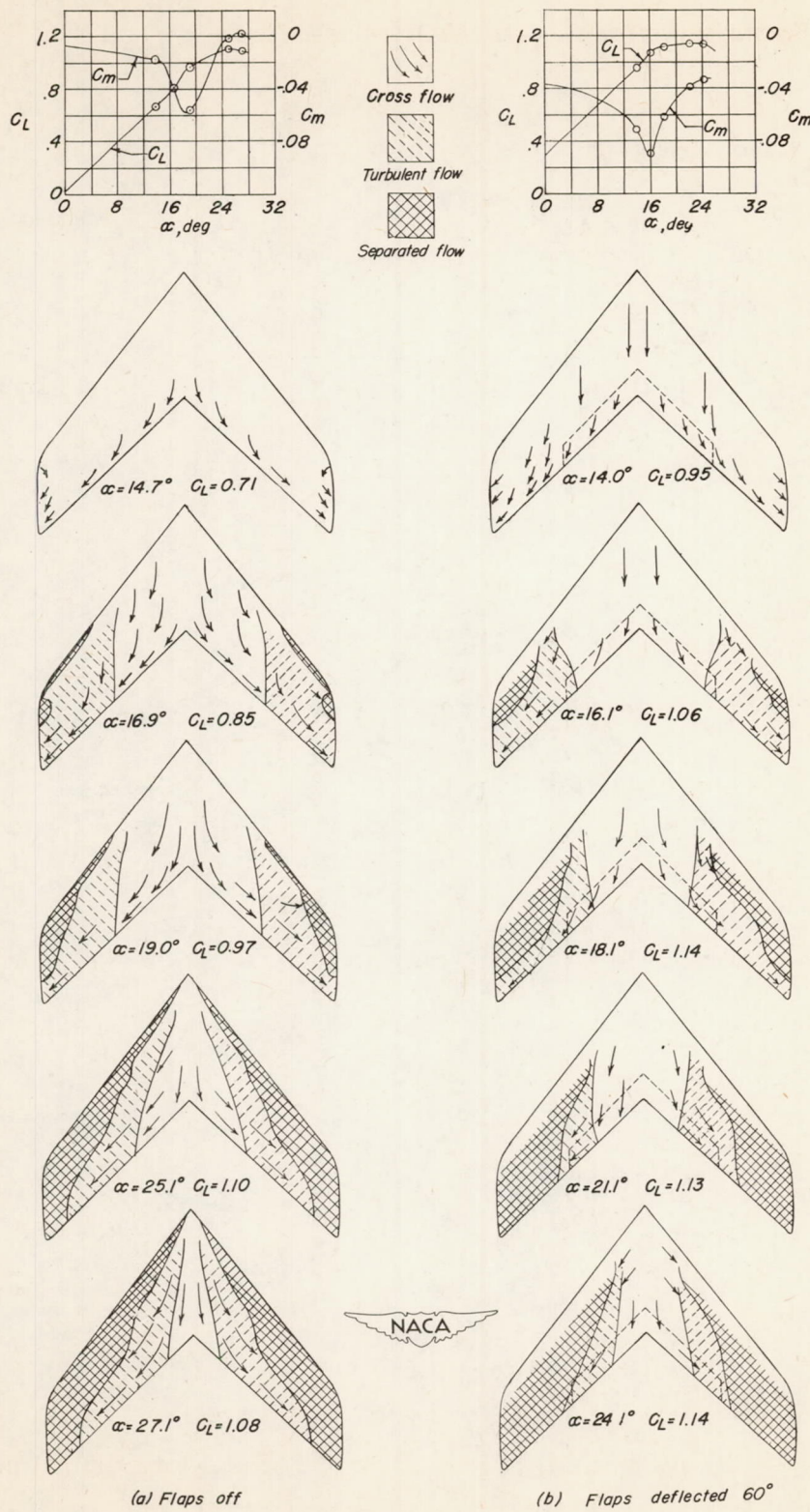


Figure 8.- Stall characteristics of a 52° sweptback wing.  $R = 6,800,000$ .

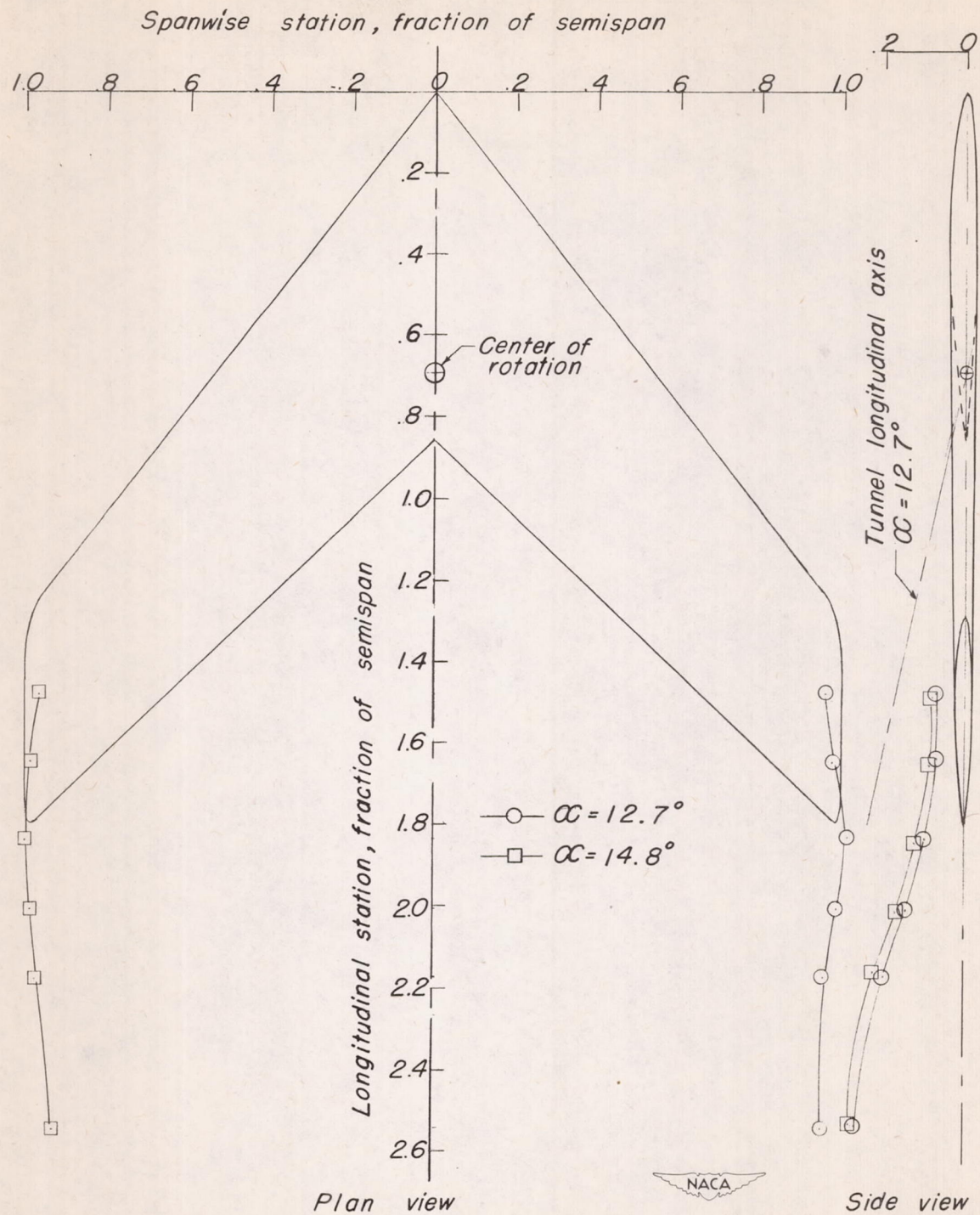


Figure 9.- Position of edge vortex core at several longitudinal stations.  
 $R = 3,600,000$ .

